

# First experimental research in low energy proton radiography\*

WEI Tao(魏涛)<sup>1)</sup> YANG Guo-Jun(杨国君) LI Yi-Ding(李一丁) LONG Ji-Dong(龙继东)  
 HE Xiao-Zhong(何小中) ZHANG Xiao-Ding(张小丁) JIANG Xiao-Guo(江孝国) MA Chao-Fan(马超凡)  
 ZHAO Liang-Chao(赵良超) YANG Xing-Lin(杨兴林) ZHANG Zhuo(张卓) WANG Yuan(王远)  
 PANG Jian(庞健) LI Hong(李洪) LI Wei-Feng(李伟峰) ZHOU Fu-Xin(周符新) SHI Jin-Shui(石金水)  
 ZHANG Kai-Zhi(张开志) LI Jin(李劲) ZHANG Lin-Wen(章林文) DENG Jian-Jun(邓建军)

Institute of Fluid Physics, China Academy of Engineering Physics, P.O. Box 919-106, Mianyang 621900, China

**Abstract:** Proton radiography is a new scatheless diagnostic tool providing a potential development direction for advanced hydrotesting. Recently a low energy proton radiography system has been developed at the Chinese Academy of Engineering Physics (CAEP). This system has been designed to use an 11 MeV proton beam to radiograph thin static objects. This system consists of a proton cyclotron coupled to an imaging beamline, which is the first domestic beamline dedicated to proton radiography experiments. Via some demonstration experiments, the radiography system is confirmed to provide clear pictures with spatial resolution  $\sim 100 \mu\text{m}$  within 40 mm field-of-view.

**Key words:** proton radiography, beamline, spatial resolution

**PACS:** 29.27.Eg **DOI:** 10.1088/1674-1137/38/8/087003

## 1 Introduction

The technique of proton radiography (pRad) was developed at LANL to use a 800 MeV proton beam as a radiographic probe for diagnostics hydrotesting research [1]. The beam optics requirements for a pRad lens system are well understood [2] and are shown schematically in Fig. 1, the different colors representing the different scattering angles within the object.

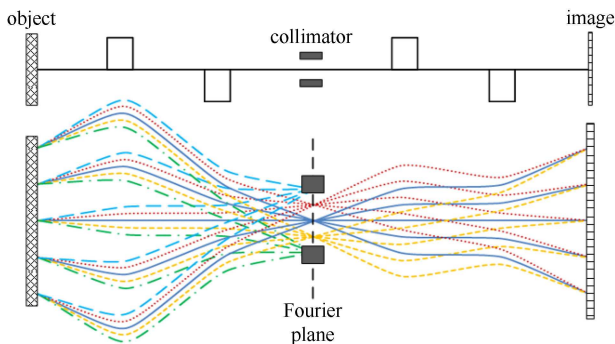


Fig. 1. (color online) Schematic diagram of a pRad lens system showing the point-to-point focus of particle trajectories (colored lines) from object to image.

There are two primary requirements for a pRad lens system [3]. First, the lens system must provide a point-

to-point focus from object to image. Second, it must form a Fourier plane, where particles can be sorted by scattering angle. With the latter requirement, particles with large scattering angles can be removed through transverse collimation at the Fourier plane. Otherwise, the object length must be suited to the beam energy, and the aperture of the lens system must be chosen to provide sufficient acceptance throughout the required field-of-view.

## 2 Low energy proton radiography system

Currently, the pRad technique is mainly used at high energy proton accelerators, for example the 800 MeV pRad at LANSCE, 24 GeV pRad at AGS [4] and 70 GeV pRad at IHEP [5]. Recent work at the Chinese Academy of Engineering Physics (CAEP) has extended this diagnostic technique to low energy proton accelerators.

### 2.1 Proton source

An 11 MeV  $\text{H}^-$  compact cyclotron used for medical radioactive isotope production is in operation [6] at the Institute of Fluid Physics, CAEP. This cyclotron is capable of providing a continuous wave beam, and the

Received 23 October 2013

\* Supported by National Natural Science Foundation of China (11205144), National Natural Science Foundation of China (11176001) and Science and Technology Development Program of China Academy of Engineering Physics (2010A042016)

1) E-mail: weitaocaep@gmail.com

©2014 Chinese Physical Society and the Institute of High Energy Physics of the Chinese Academy of Sciences and the Institute of Modern Physics of the Chinese Academy of Sciences and IOP Publishing Ltd

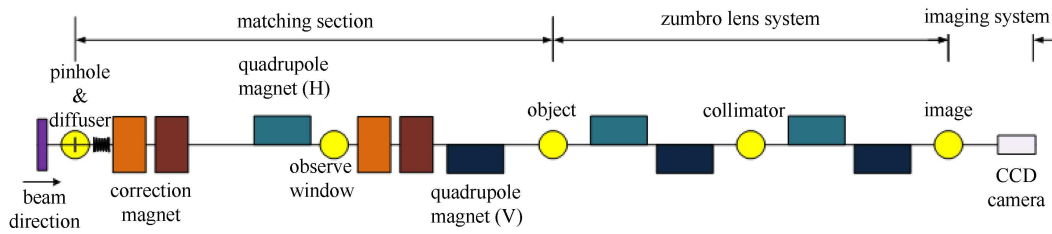


Fig. 2. (color online) Layout of 11 MeV low energy pRad beamline.

average current is about 50  $\mu\text{A}$ . The negative hydrogen beam is converted to a proton beam through carbon stripping foil.

### 2.2 pRad imaging beamline

Fig. 2 shows the layout of the 11 MeV low energy pRad imaging beamline, and Fig. 3 shows the twiss parameters. Firstly, the proton beam passes through the matching section to be modulated for the correlation between particles' transverse displacement and angle deviation [3]. Then the modulated beam penetrates a thin object while keeping the multiple Coulomb scattering (MCS) angle and energy loss small enough to allow good spatial resolution. Finally, the beam passes through a Zumbro lens system and arrives at the scintillation detector.

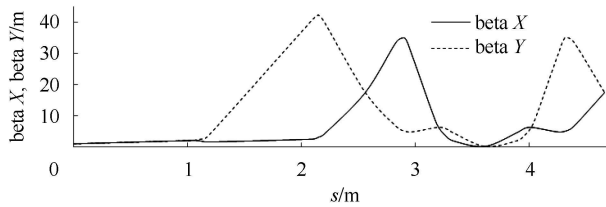


Fig. 3. Twiss parameters of 11 MeV low energy pRad beamline.

The required phase space correlations are provided by the matching section just upstream of the object. Moreover, this section must also expand the beam's transverse size to fully illuminate the field-of-view. The proton beam from the cyclotron first passes through a pinhole of 1 mm diameter, so the beam is truncated and the central part preserved. The preserved proton beam passes through a 20  $\mu\text{m}$  aluminum diffuser to have a small angular divergence and then passes through a set of magnets, which introduces a correlation between the radial position in the object plane and its angle. Fig. 4 shows the evolution diagram of a low energy proton beam in the matching section. Through the matching section, the proton beam is well modulated and the width is enlarged long enough to illuminate the whole object.

The Zumbro lens system consists mainly of four identical quadrupole magnets, and after proper arrangement,

can obtain one-to-one imaging. The aperture is 60 mm and the chromatic coefficients [7]  $R'_{12}$  (for  $x$  direction) and  $R'_{34}$  (for  $y$  direction) are both about 2.8 m. The collimator adopts a hole-type structure, with the inner hole for the proton beam to travel through, while the outer layer is made of aluminum which is thick enough to stop the proton beam. With the collimator, one can limit the transmitted particles to only those with a MCS angle less than the cut angle.

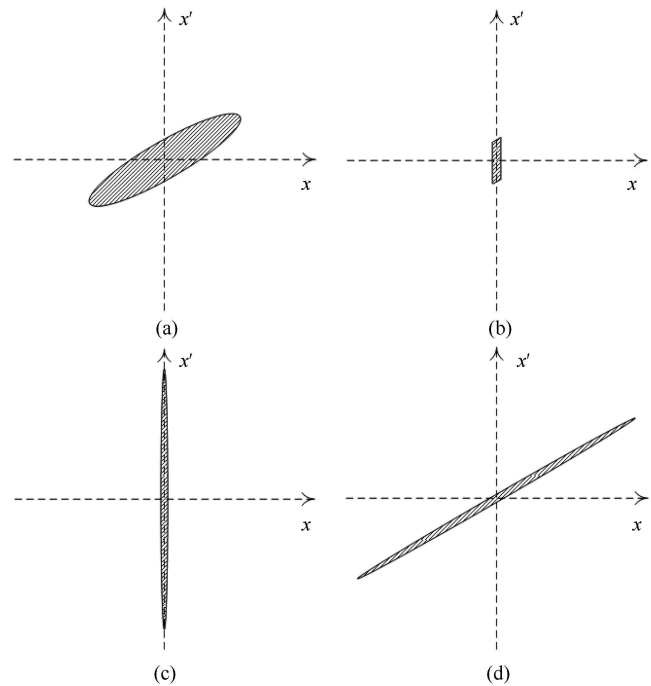


Fig. 4. Evolution diagram of transverse phase space. (a) is the initial horizontal phase space, (b) is the beam distribution after the pinhole, (c) is the case after the diffuser and (d) is the case at the object plane.

The imaging system is made of a piece of LSO scintillator followed by a CCD camera. Visible light is generated when the proton beam hits the scintillator, and is collected by a CCD camera.

### 3 Radiographic performance

The low energy pRad system was commissioned in June 2013 at the Institute of Fluid Physics. The imaging beamline performed as designed. Detailed measurement of spatial resolution was collected by studying a “zebra crossing” image, as shown in Fig. 5. Stripes of different widths were printed on aluminum foil by a laser printer, with the partition length equal to the width of each stripe. There are four kinds of stripes in Fig. 5, with widths 1 mm, 0.5 mm, 0.2 mm and 0.1 mm respectively. In order to obtain a clear image, the beam distribution should be uniform in the  $x$ - $y$  plane, but this is hard to achieve. In fact, we can remove the influence of the beam’s nonuniform distribution using the original radiograph divided by the beam radiograph. Moreover, the noise introduced by the CCD should also be removed.

As shown in Fig. 5, the spatial resolution of the 11 MeV low energy pRad is then better than 0.1 mm.

The spatial resolution can also be estimated by the width of the rising or falling edge of the interface. Fig. 6 shows the transmitting rate and its differential curve corresponding to the 1 mm stripes. Here  $s$  represents the vertical displacement along the 1 mm stripes, and  $\tau$  represents the transmitting rate. The fitted Gaussian curve in the right-hand figure matches the square data points very well, and the FWHM is 0.1 mm.

In addition to detailed resolution measurements some familiar items were radiographed as a demonstration of the sensitivity and high resolution capabilities of the radiography system. A radiograph of cicada wings is shown in Fig. 7. The significant contrast shown in this radiograph demonstrates the extreme sensitivity of low energy pRad system to objects with thin areal densities.

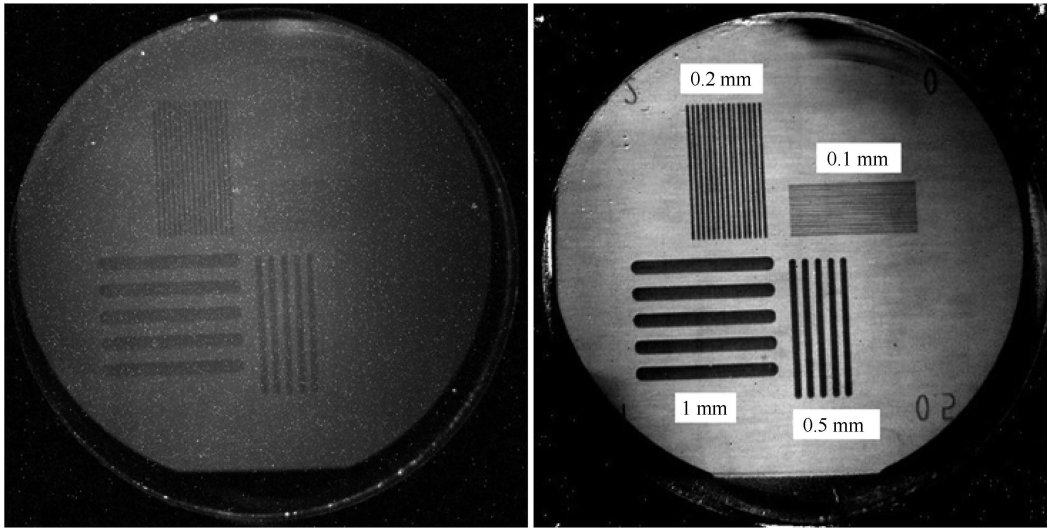


Fig. 5. Low energy pRad image of the stripes on aluminum foil. The left-hand side is the original radiograph, the right-hand side is the image after removing the influence of noise and nonuniform beam distribution.

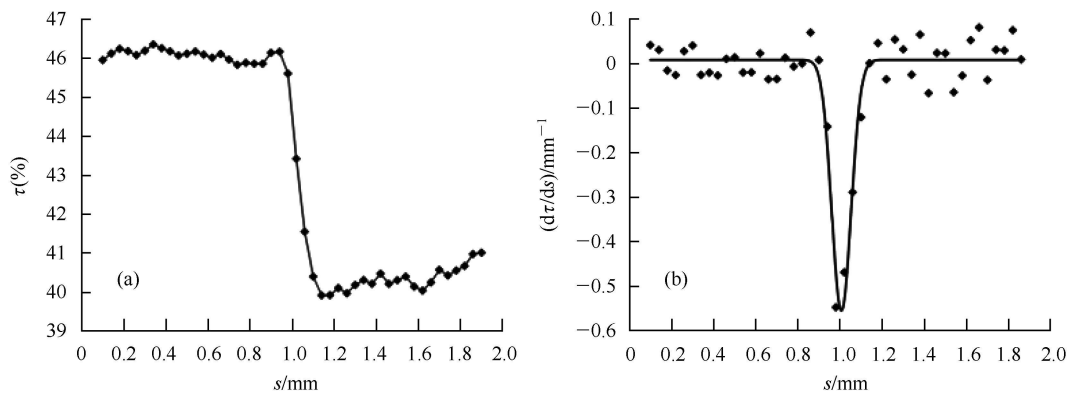


Fig. 6. The transmitting rate (a) and its differential curve (b) corresponding to the 1 mm stripes. The squares are data points, the line in the right-hand figure is the fitted Gaussian curve.

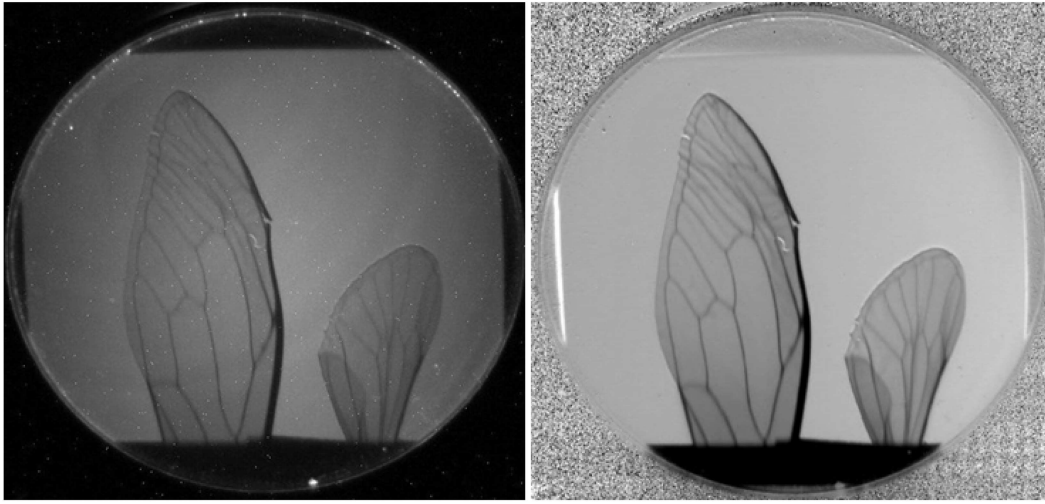


Fig. 7. Low energy pRad image of the cicada wings. The left-hand side is the original radiograph, the right-hand side is the image after removing the influence of noise and nonuniform beam distribution.

## 4 Conclusion

An 11 MeV low energy pRad system has been designed and built. This system can provide scatheless diagnosis for static objects with  $0.001\text{--}0.03\text{ g/cm}^2$  densities with spatial resolution of  $\sim 100\text{ }\mu\text{m}$ .

Many aspects of the radiography system can be im-

proved, for example, increasing the beam current for performing dynamic diagnosis, and reducing the jitter of the proton beam to improve the image quality.

For the present, the radiography ability is mainly limited by the optical receiving system, so the upgrade to the radiography system which can most likely give significant improvement in the spatial resolution is to use a magnifying Zumbro lens system [8].

## References

- 1 King N S P, Ables E, Ken Adams et al. *NIMA*, 1999, **424**: 84–91
- 2 WEI Tao, YANG Guo-Jun, LONG Ji-Dong et al. *Chinese Physics C*, 2013, **37**(6): 068201
- 3 WEI Tao, YANG Guo-Jun, LONG Ji-Dong et al. *Chinese Physics C*, 2012, **36**(8): 792–796
- 4 Morris C L, Ables E, Alrick K R et al. *Journal of Applied Physics*, 2011, **109**(10): 104905
- 5 Burtsev V V, Lebedev A I, Mikhailov A L et al. *Combustion, Explosion, and Shock Waves*, 2011, **47**(6): 627–638
- 6 WEI Tao, YANG Guo-Jun, HE Xiao-Zhong et al. *High Power Laser and Particle Beams*, 2012, **24**(9): 2193–2197 (in Chinese)
- 7 HE Xiao-Zhong, YANG Guo-Jun, LIU Chen-Jun. *High Power Laser and Particle Beams*, 2008, **20**(2): 297–300 (in Chinese)
- 8 YANG Guo-Jun, ZHANG Zhuo, WEI Tao et al. *Chinese Physics C*, 2012, **36**(3): 247–250